Dark Matter Equilibria in Galaxies and Galaxy Systems

Andrea Lapi

Dip. Fisica, Univ. degli Studi di Roma “Tor Vergata”, Italy
Astrophysics Sector, SISSA/ISAS, Trieste, Italy

UNIVERSITA' degli STUDI di ROMA TOR VERGATA

in collaboration with: A. Cavaliere (UniRoma2, Italy)
R. Fusco-Femiano (INAF-IASF Roma, Italy)

Overview

Introduction

- <u>Dark Matter (DM) cosmogony in a couple of slides</u>

  - Initial DM density perturbations grow by gravitational instability, at first kept in check by the cosmic expansion, then enforced to collapse when local gravity prevails (e.g., Peebles 93) .

  - A slightly overdense region expands more slowly than its surroundings, progressively detaches from the Hubble flow, halts, turns around, collapses, and eventually virializes to form a DM halo in equilibrium under self-gravity.

  - Amplitude of more massive perturbation in the initial density field is smaller, so they form later on: hierarchical clustering .

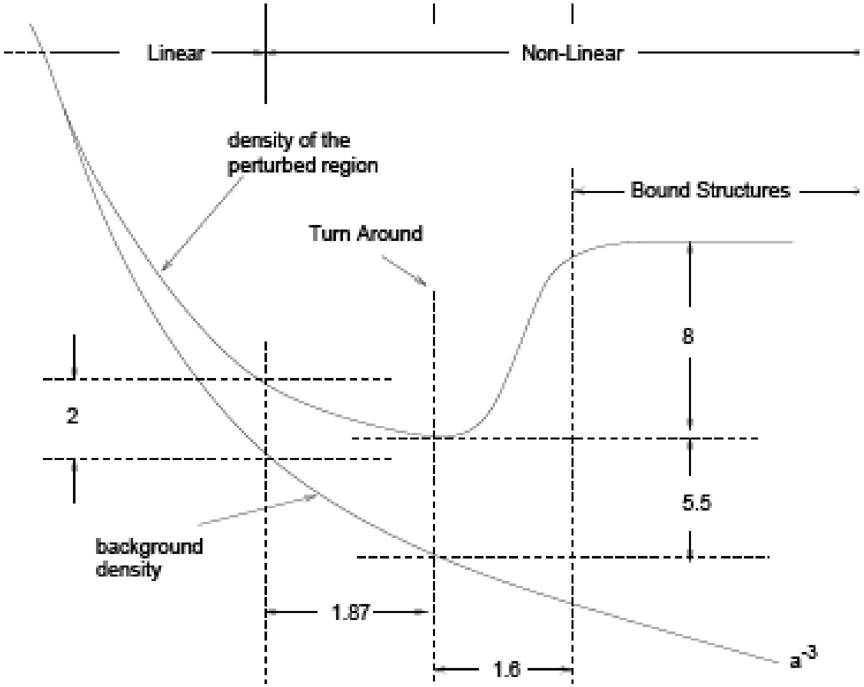

Figure from Padmanabhan 02

Introduction

- N-body simulations soon confirmed this picture (e.g., White86) and resolved it to a fine detail, adding two important blocks of info (e.g., Springel+06).

- First, the halo growth actually occurs through multiple stochastic merging events with other clumps of sizes comparable (major mergers) or smaller (minor mergers), down to nearly smooth accretion.

  Rem. This behavior is usually visualized according to a computational structure called merger tree.

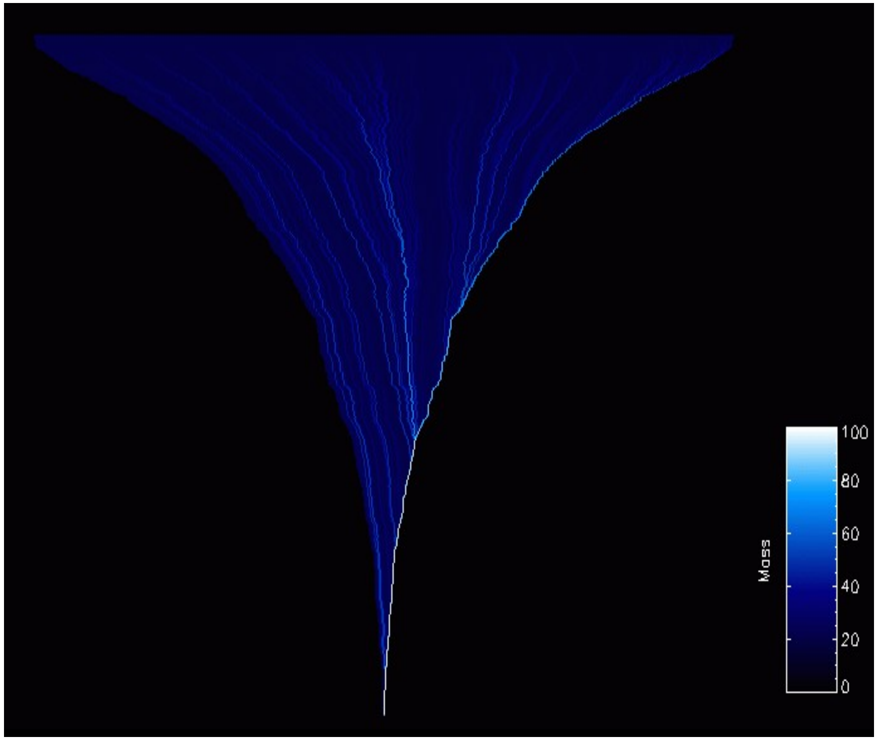

Figure from Menci+06

Introduction

- Second, at any stage the density profile in the virialized halos is empirically described by the NFW formula (Navarro+97)

$$\boxed{\rho(r) \propto \frac{1}{\hat{r}\,(1+\hat{r})^2}} \qquad \hat{r} \equiv \frac{r}{r_{-2}}$$

This is scale-invariant apart from minor deviations related to the mild mass dependence of the present concentration parameter (e.g., Bullock+01, Wechsler+02, Macciò+08, Klypin+10)

$$c \equiv \frac{R}{r_{-2}} \propto M^{-0.13}$$

with the limit c>4 at the high mass end.

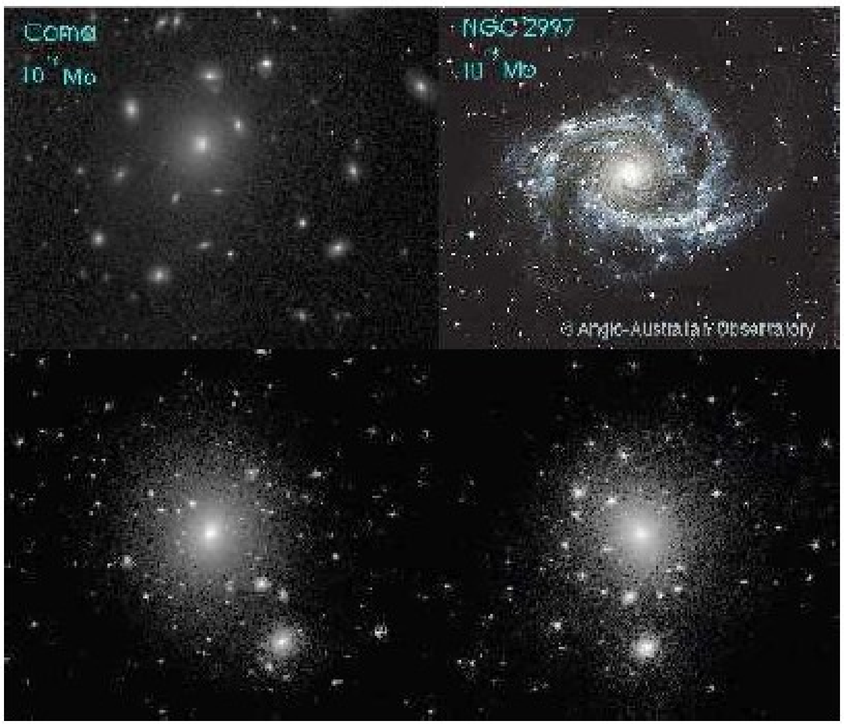

Figure from www.nbody.net, B. Moore

Introduction

Recent pieces of news

- Intensive high-resolution N-body simulations (Zhao+03, Diemand+07, Hoffman+07, Ascasibar & Gottloeber 08, Gao+08, Stadel+09, Navarro+10) have recently focused on the halo development, with 3 main outcomes.

- First, the halo growth comprises two stages: an early fast collapse including a few violent major mergers building up the halo 'body' (cf. r_{-2}); and a later slow accretion, when the body is almost unaffected while the outskirts develop from the inside-out by minor mergers and smooth mass additions. The transition occurs when the circular velocity $v_c^2=GM/R$ attains its maximum along the growth history.

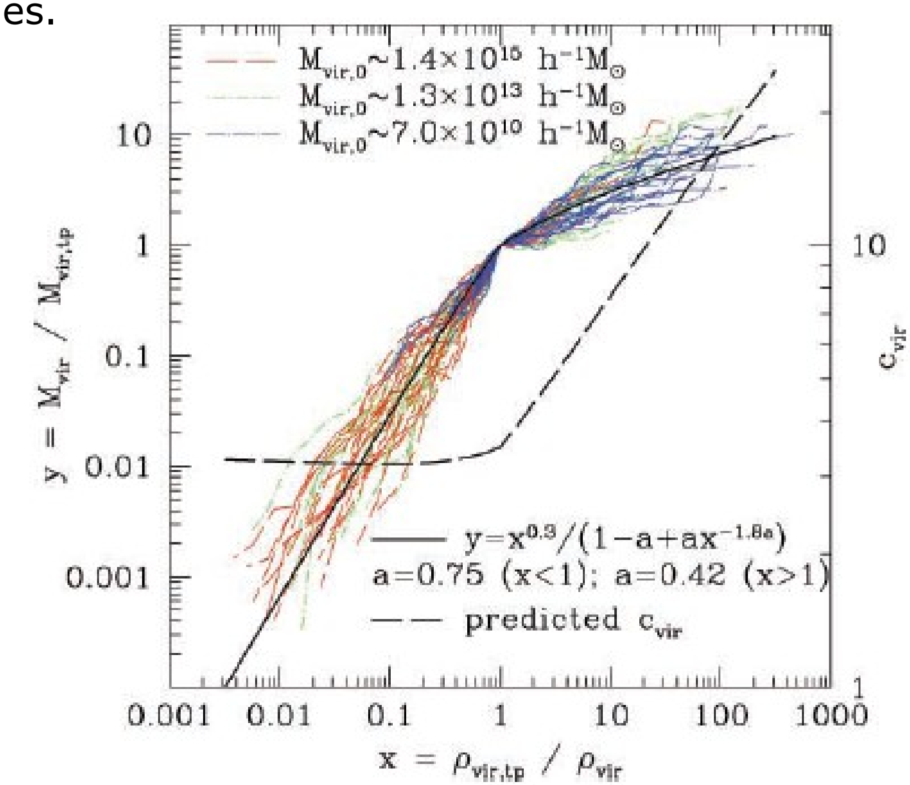

Figure from Zhao+03

Introduction

- Second, a universal feature of the ensuing quasi-equilibrium structure is constituted by the powerlaw correlation

$$\boxed{K \equiv \frac{\sigma^2}{\rho^{2/3}} \propto r^\alpha}$$

with $\alpha \sim 1.25 - 1.3$. This combines density and (radial, total) velocity dispersion in the form of a DM 'entropy' (or 'adiabat') formally analogous to the true thermodynamic entropy of a gas in thermal equilibrium.

- Rem. Equivalently, a pseudo coarse-grained phase-space density is often considered

$$Q \equiv K^{-3/2}$$

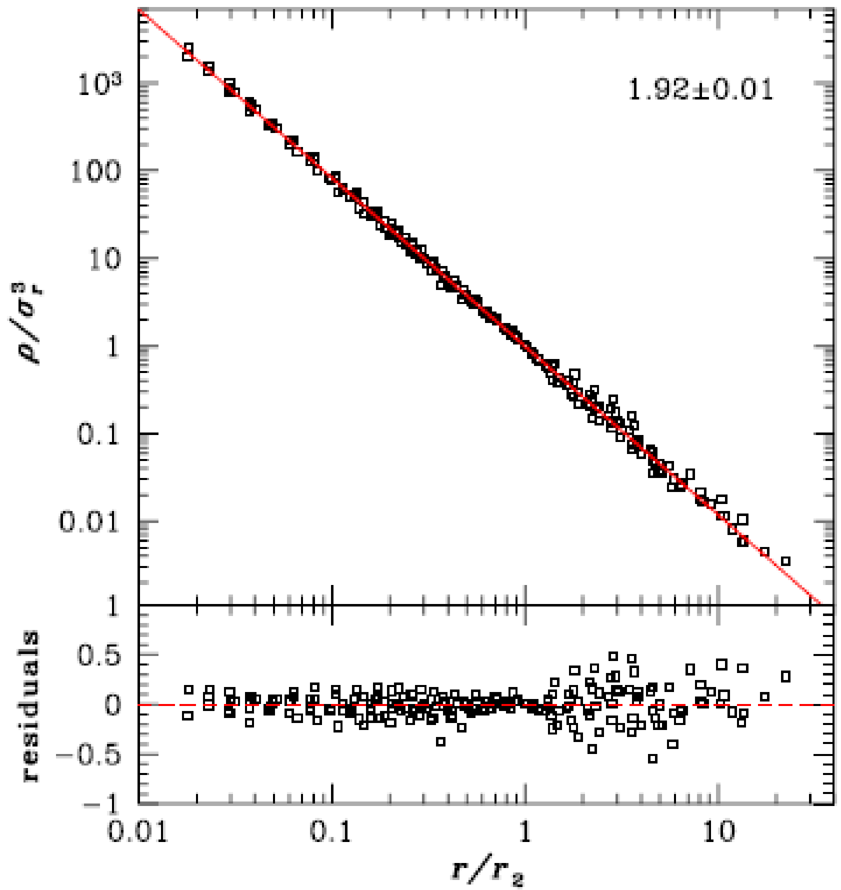

Figure from Dehnen & McLaughlin 05

Introduction

- Third, the density profiles of simulated halos are best fitted in terms of the classic Sersic-Einasto models (Sersic 63, Einasto 65, Prugniel & Simien 97):

$$\rho(r) \propto \hat{r}^{-\tau}\, e^{-\frac{2-\tau}{\eta}\,\hat{r}^{\eta}}$$

with parameters $\tau<0.9$ and $\eta \sim 0.2$.

- Rem. These models are also known to provide very good representation of the stellar mass profile in early-type galaxies (e.g., Kormendy+09), but still lack of an astrophysical understanding...

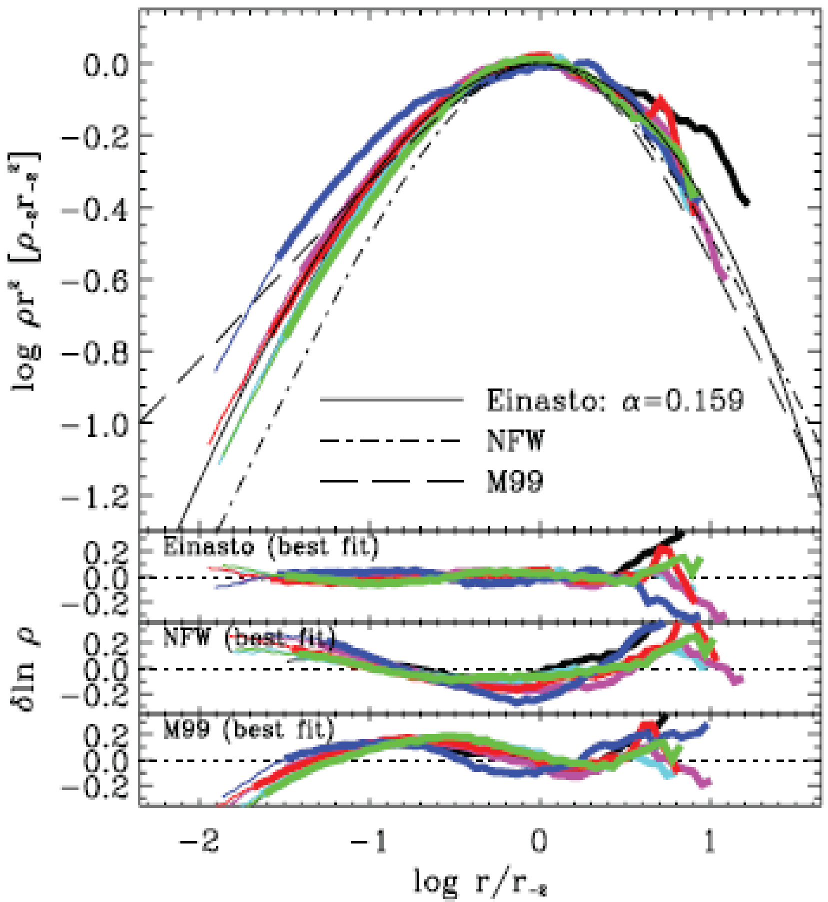

Figure from Navarro+10

Two-Stage Development of DM Halos

Origin of the DM entropy slope

- The entropy slope may be derived from the classic theory of self-similar collapse (see Fillmore & Goldreich 84, Austin+05, Lu+06, LC09a). Consider a perturbation with powerlaw shape

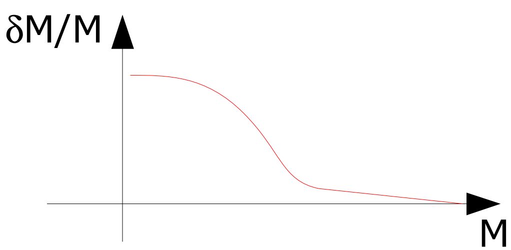

$$\frac{\delta M}{M} \propto M^{-\epsilon}$$

$\epsilon \ll 1$ top-hat

$\epsilon \lesssim 1$ point-mass

$\epsilon \gg 1$ wings

- A perturbation will collapse when δM/M attains the critical threshold 1.686 $D^{-1}(t)$ in terms of the growth factor $D(t) \sim t^{d}$ (with $d \sim 2/3 \rightarrow 1/2$ for z lowering toward 0), so that ε also controls the mass growth as

$$M(t) \propto D^{1/\epsilon}(t) \propto t^{d/\epsilon}$$

$\epsilon \ll 1$ fast collapse

$\epsilon \lesssim 1$ transition

$\epsilon \gg 1$ slow accretion

Two-Stage Development of DM Halos

- Each mass shell will collapse down to a radius $R \propto \frac{R_{\rm in}}{\delta M/M} \propto M^{\epsilon+1/3}$

  so that by dimensional arguments one obtains the scaling laws

$$\rho \propto \frac{M}{R^3} \propto M^{-3\,\epsilon}$$

$$\sigma^2 \propto \frac{M}{R} \propto M^{2/3-\epsilon}$$

$$\Rightarrow \quad K \propto \frac{\sigma^2}{\rho^{2/3}} \propto M^{\epsilon+2/3}$$

- Assuming that particles of each collapsed shell spend most of the time at the apocenter of their orbits, i.e., that the apocenters stratify (see Bertschinger 1985), one can recast the above in terms or R to find

$$K \propto R^{\alpha} \qquad \text{with} \qquad \boxed{\alpha = \frac{2+3\,\epsilon}{1+3\,\epsilon}} \rightarrow \begin{cases} 2 & \epsilon \ll 1 \\ \approx 1.3 & \epsilon \lesssim 1 \\ 1 & \epsilon \gg 1 \end{cases}$$

  in agreement with simulations!

Two-Stage Development of DM Halos

- This heuristic computation can be checked and refined in terms of the halo average growth histories, obtained from integrating for M(t) the differential equation

$$\boxed{\dot{M}(M,t) = \int_0^M dM'\,(M-M')\,\frac{\mathrm{d}^2 P_{M'\to M}}{\mathrm{d}M'\mathrm{d}t}}$$

where the growth kernel under ellipsoidal collapse (see Sheth & Tormen 02, Zhang+08) incorporates the full cosmology, and the detailed cold DM power spectrum.

- The resulting evolutionary tracks render the peaked behavior of $v^2_c(t)$ in remarkable agreement with both simulations (e.g., Zhao+03, Diemand+07) and semyanalitic computations based on the simpler EPS theory (e.g., Neistein+06, Li+07).

- The transition redshifts are found to be lower for larger current body masses, as expected in a hierarchical cosmogony; note that all that holds on the average, but considerable variance arises from the stochastic nature of the single growth histories.

Two-Stage Development of DM Halos

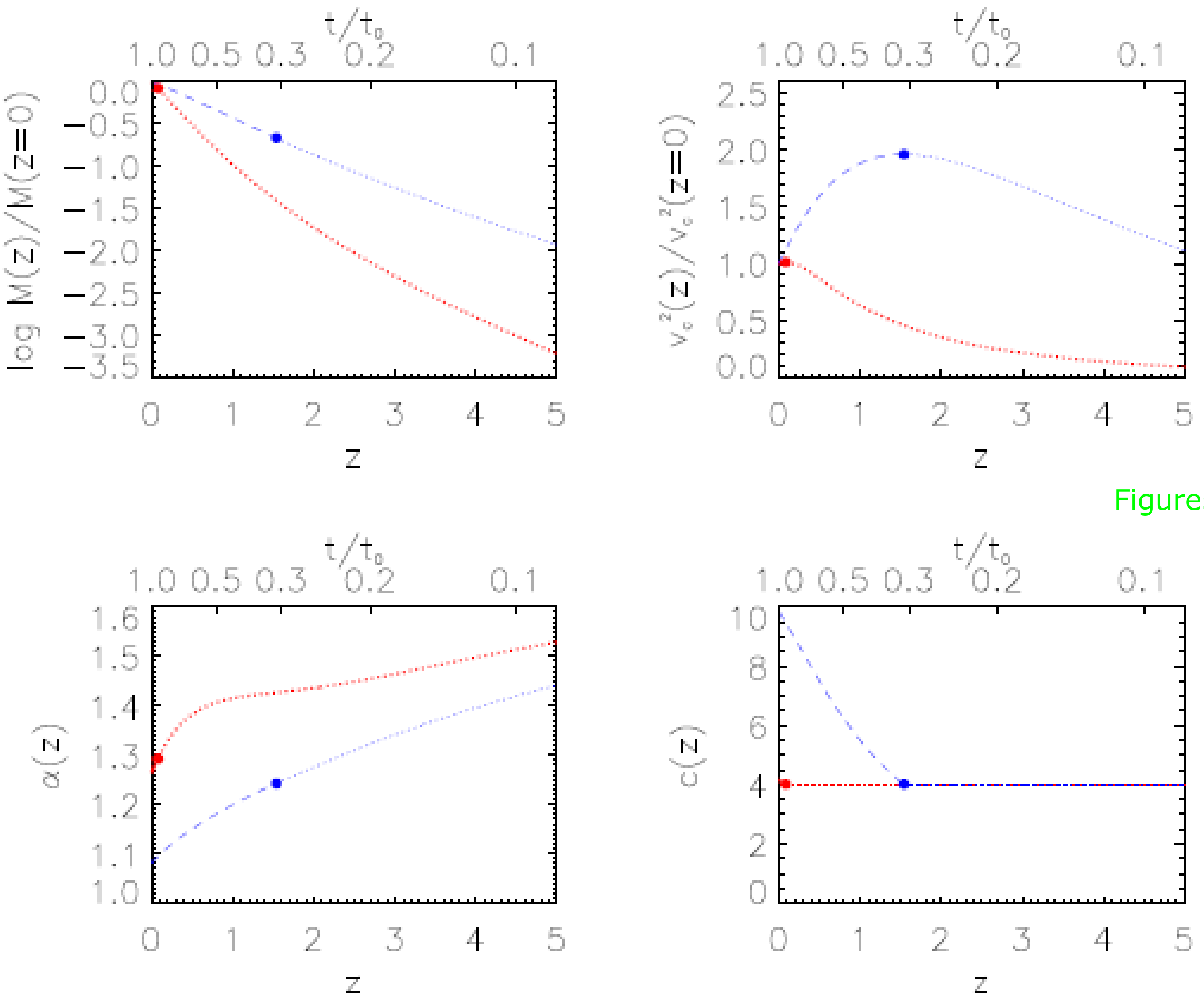

Figures from LC09b

UNIVERSITA' degli STUDI di ROMA TOR VERGATA

Equilibrium Structure of DM Halos

- α-profiles from Jeans Equation
  - The static equilibria of the DM halos obey the classic Jeans equation:

$$\frac{1}{\rho}\frac{\mathrm{d}(\rho\,\sigma_r^2)}{\mathrm{d}r} = -\frac{GM(<r)}{r^2} - \frac{2\beta\,\sigma_r^2}{r}$$

The radial pressure term can be expressed as $\rho\ \sigma_r^{\ 2} \sim K\ \rho^{5/3} \sim r^{\alpha}\ \rho^{5/3}$; any anisotropy is included via the standard parameter $\beta = 1 - \sigma_\theta^{\ 2}/\sigma_r^{\ 2}$ (see Binney 78).

  - In terms of the density slope $\gamma(r) = -\mathrm{dlog}\ \rho\ /\mathrm{dlog}\ r$, Jeans may be recast into the form

$$\boxed{\gamma = \frac{3}{5}\,(\alpha + \frac{v_c^2}{\sigma_r^2}) + \frac{6}{5}\,\beta\ ;}$$

when supplemented with the mass definition $M(<r) = 4\pi \int dr\ r^2\ \rho(r)$ entering $v^2_{\ c} = GM/R$, this constitutes an integro-differential equation for $\rho(r)$, that by double differentiation reduces to a handy autonomous 2nd order equation for $\gamma(r)$, see e.g. Austin+05.

Equilibrium Structure of DM Halos

- The study of the solution space for the Jeans Equation in the isotropic case yields that a physical 'α-profile' exists for every $\alpha \leq 35/27 = 1.\overline{296}$ (Dehnen & McLaughlin 05; LC09a); this condition guarantees the corresponding density run to be monotonically steepening outwards and to satisfy regular boundary conditions both at the center (round minimum of the potential with finite energy density) and in the outskirts (finite mass).

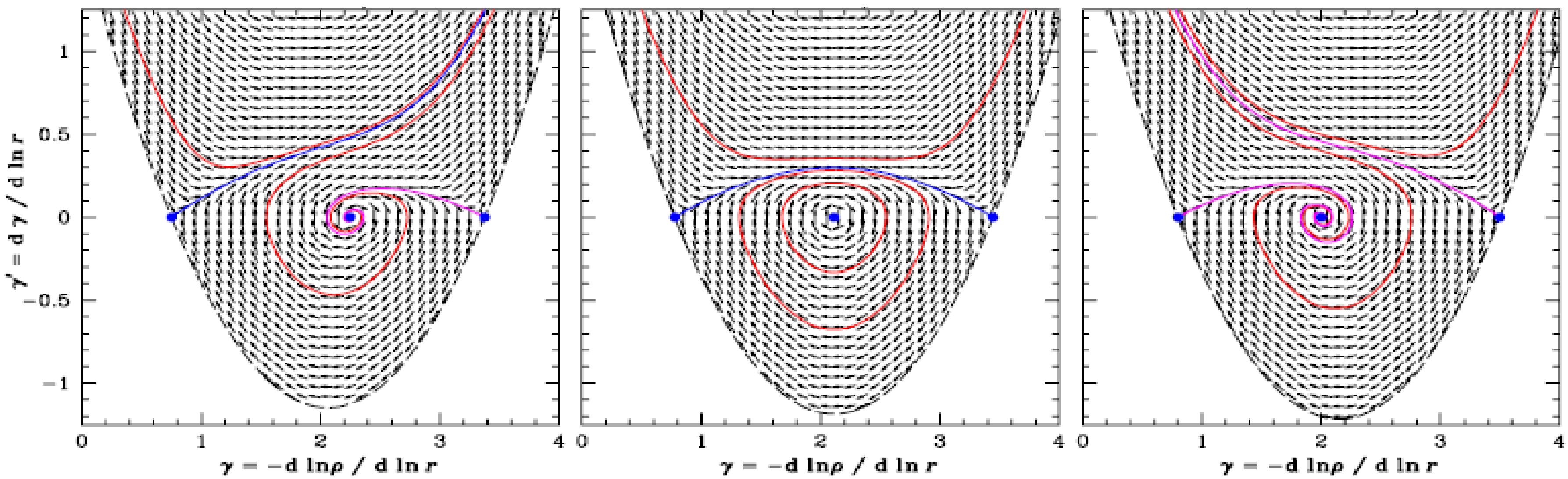

Figure from Dehnen & McLaughlin 05

Equilibrium Structure of DM Halos

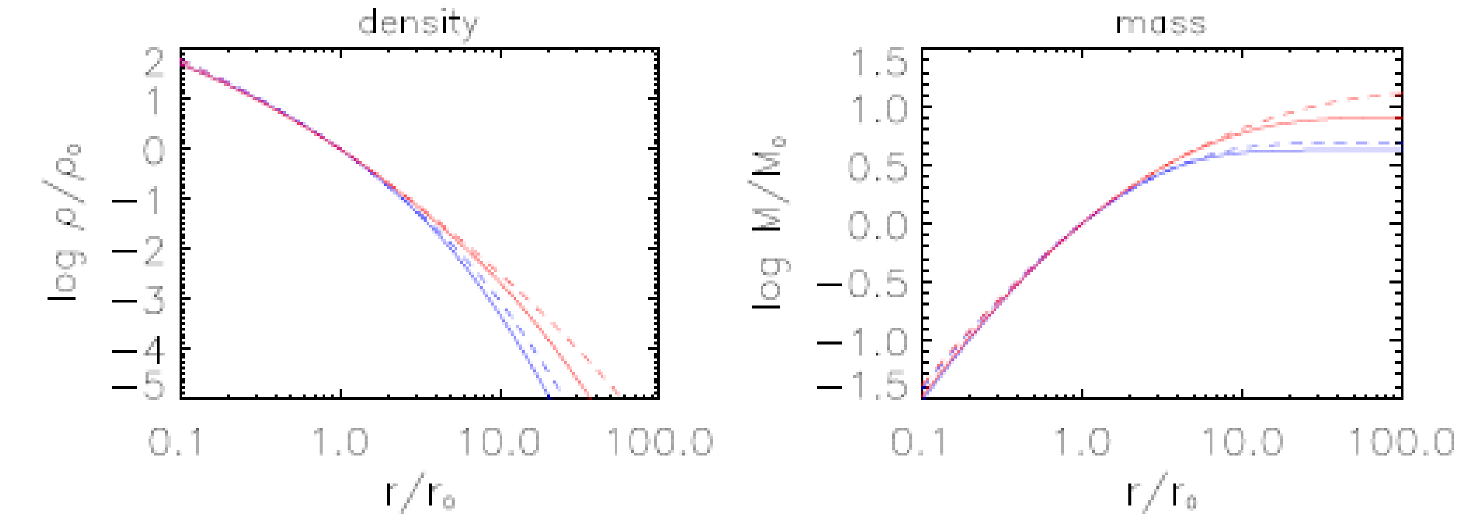

Figures from LC09b

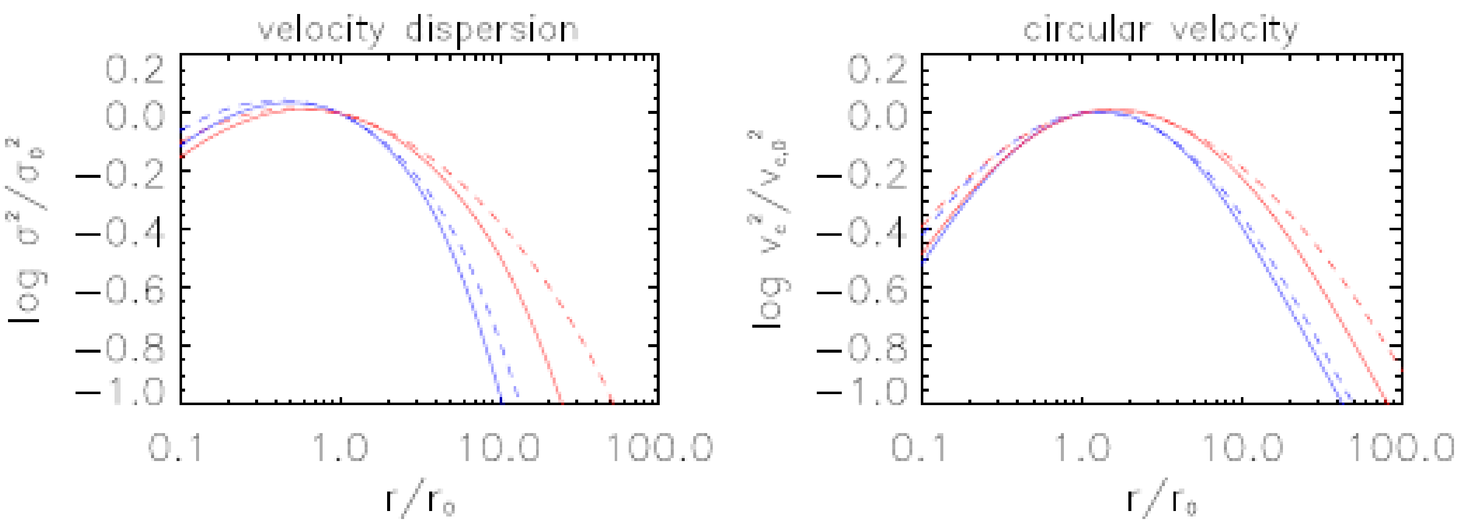

Equilibrium Structure of DM Halos

- The α-profiles can be extended to anisotropic conditions (see LC09b). It is clear from Jeans that the anisotropy term will flatten/steepen the density run for negative/positive β. The former condition is expected in the inner region, where tangential component develop from the angular momentum barrier. Moving outwards, radial motions are expected to prevail, so raising up β. But outward of the first DM caustics, β is expected to decrease. Numerical simulations confirm such a picture and (Hansen & Moore 06, Navarro+10) indicate the linear approximation

$$\boxed{\beta(r) \approx \beta(0) + \beta' \left[\gamma(r) - \gamma_a\right]}$$

to hold with $\beta(0)>\sim -0.1$, $\beta' \sim 0.2$, and $\beta < 0.5$.

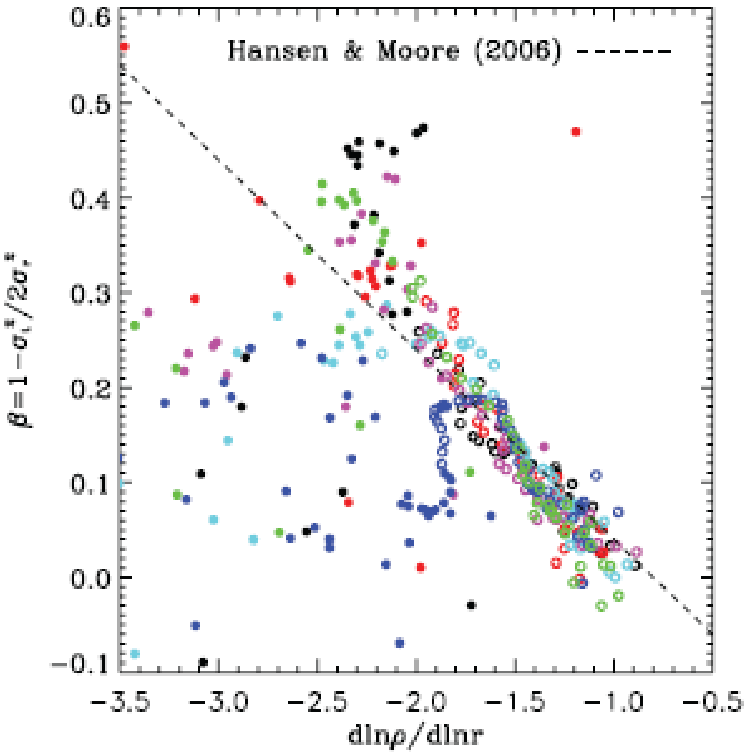

Figure from Navarro+10

Equilibrium Structure of DM Halos

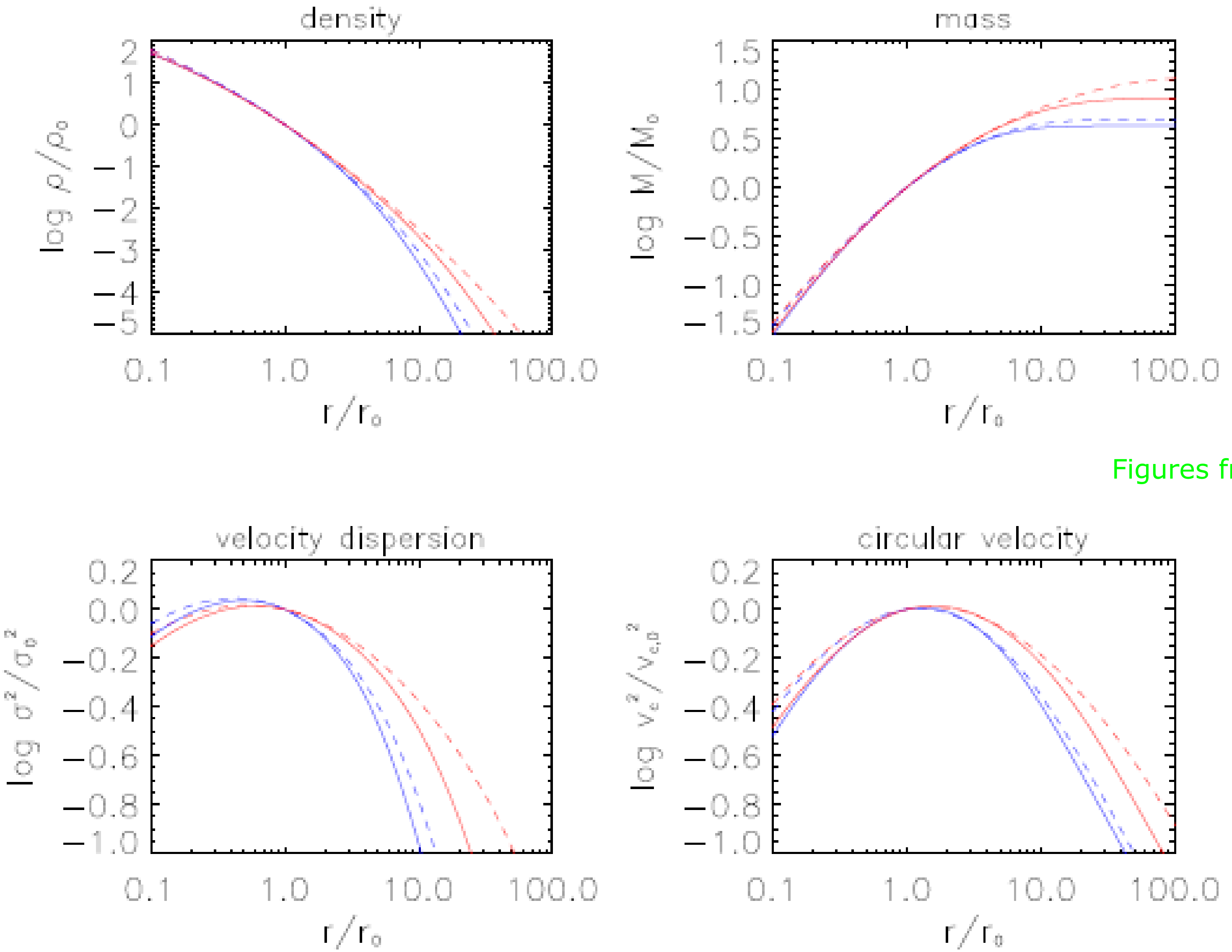

Figures from LC09b

α-Profiles at Work (I): Gravitational Lensing

- Probing the Halo Structure

- LC09b tested the α-profiles against the recent, extensive gravitational lensing (GL) observations of the cluster A1689 that join strong and weak lensing data to cover scales from 0.1 to 2.1 Mpc, the latter being close to the virial radius of the cluster. The GL data may be recast in terms of projected surface density

$$\boxed{\Sigma(s) = 2\int_s^{R_v} \mathrm{d}r\, \frac{r\,\rho(r)}{\sqrt{r^2 - s^2}}}$$

- The fits of our profiles to the GL data at given $\alpha \sim 1.27$ crucially depend on the concentration c; it is found that at the minimum χ^2 they require for the α-profiles lower concentrations than NFW, while they perform comparably or better owing to their intrinsically flatter/steeper central/outer structure.

α-Profiles at Work (I): Gravitational Lensing

Results of the Fits to the Surface Density of A1689

Reference in Figure 3	α	$\beta(0)$	c	χ^2/dof
NFW	...	...	$12.2^{+3.2}_{-2.7}$	$7.94/(26-2)$
$\alpha \geqslant 1.25$, $\beta(0)=0$	$1.25^{+0.03}$	0	$10.7^{+3.2}_{-2.5}$	$8.78/(26-3)$
$\alpha \geqslant 1.25$, $\beta(0) \geqslant -0.1$	$1.25^{+0.04}$	$-0.1^{+0.09}$	$11.6^{+2.8}_{-2.4}$	$6.55/(26-4)$
No priors	$1.18^{+0.09}_{-0.13}$	$-0.15^{+0.23}_{-0.21}$	$12.4^{+2.2}_{-2.1}$	$4.13/(26-4)$

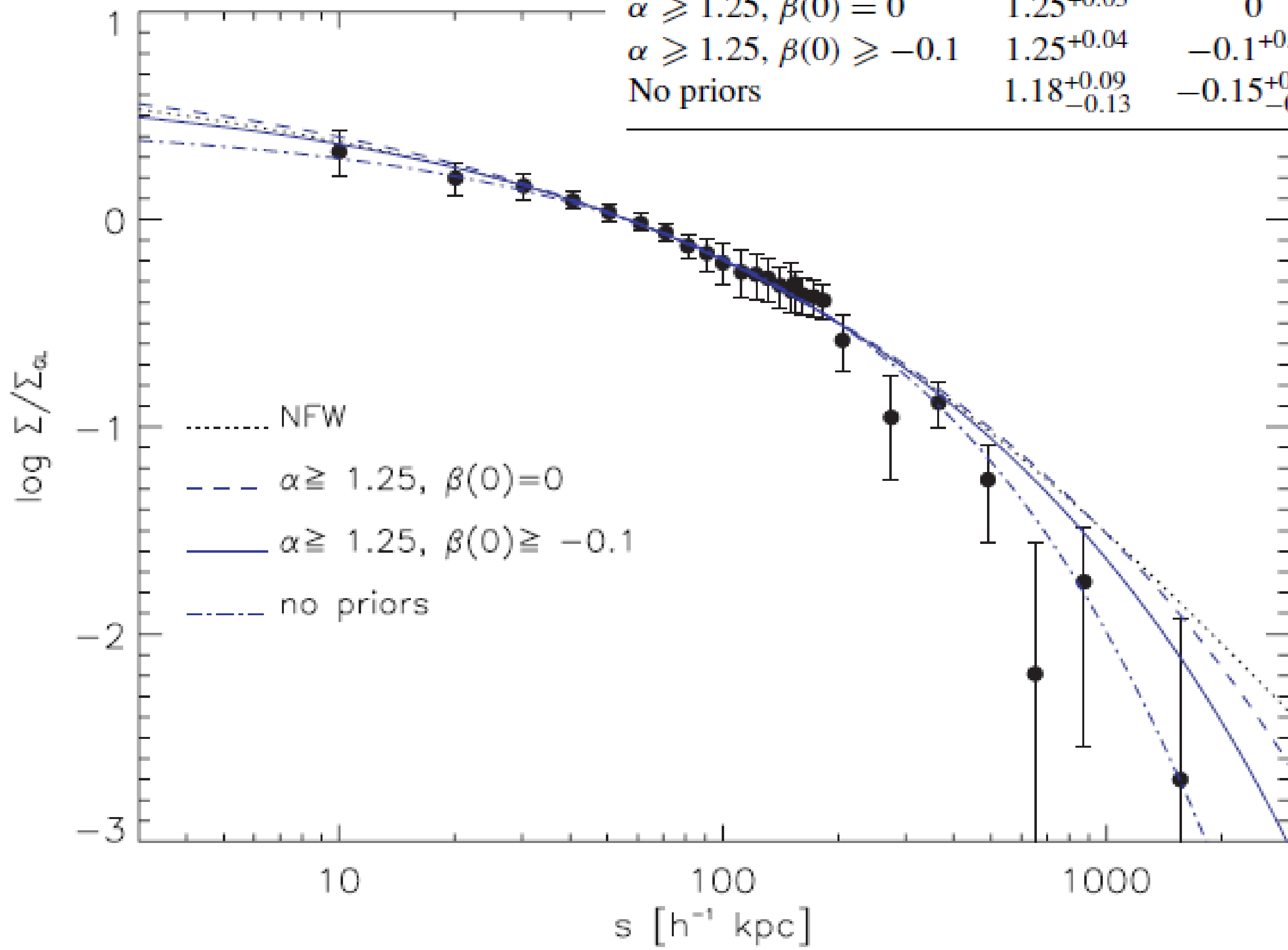

Figure from LC09b

α-Profiles at Work (I): Gravitational Lensing

Probing the Halo Development

- Note that balanced fits to the surface density in A1689 require c~10 (and even more with NFW); these values are signicantly higher than c~5 expected from the average evolutionary history of a massive cluster in the standard ΛCDM cosmogony.

- In fact, the concentration also constitutes an indicator of the halo dynamical age. According to the halo two-stage development, after the transition at z_t from fast collapse to slow accretion, the concentration evolves according to

$$c = 3.5\,\frac{H(z_t)}{H(z_{\rm obs})} \approx 3.5\frac{1+z_t}{1+z_{\rm obs}}$$

so that on the average present values c ~ 5 apply to cluster halos that had their transition at z_t <~ *0.5*, while values up to c ~ 10 apply to Milky Way sized halos that had their transition at z_t <~ *2.*

α-Profiles at Work (I): Gravitational Lensing

- To explain the high concentration of A1689, with our semyanalitic approach to the halo development we compute variant histories biased toward early times, in particular the one associated with the `main progenitor' that constitutes the main branch in a merging tree.

- Compared with the average, this history features a higher transition redshift z_t~1.5 (vs. z_t~0.2), a less massive body with 2 10^{14} M_{sun} (vs. 10^{15} M_{sun}), and currently extended outskirts (vs. nearly none). The result is a higher concentration c~4 $(1+z_t)$ ~10 (vs. c~4). The occurrence of such biased halos relative to the average is found to be 1 : 8.

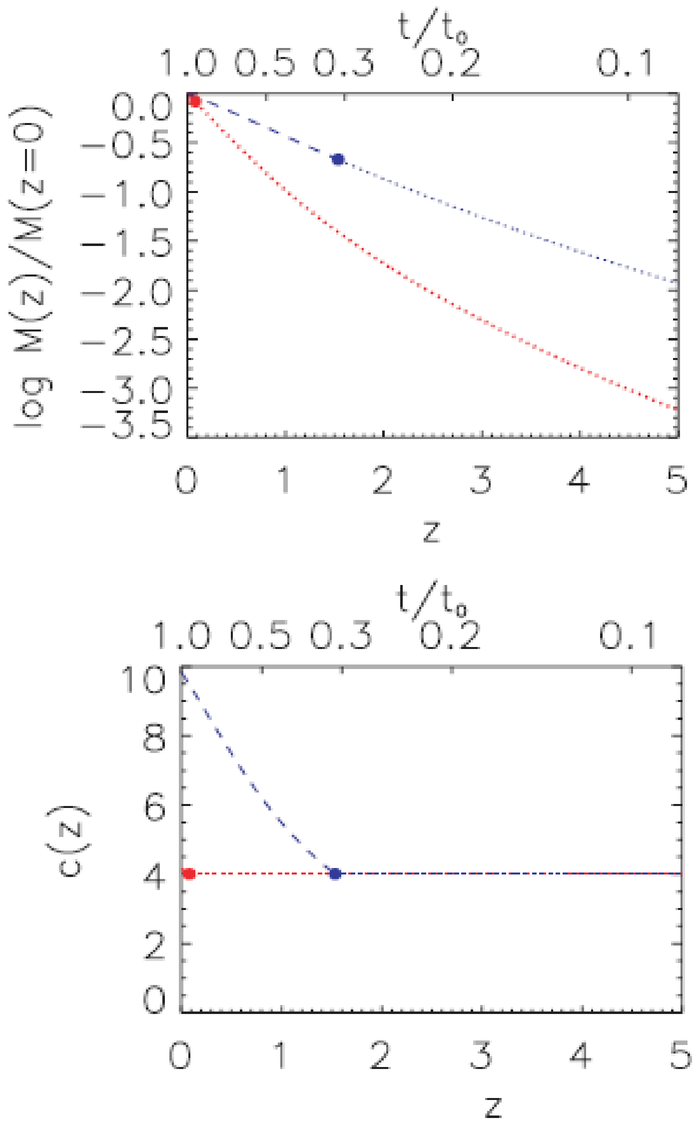

Figure from LC09b

α-Profiles at Work (I): Gravitational Lensing

- The halos produced by strongly biased histories also provide sharp GL data; in fact, observations of strong GL tend to focus on cases with centrally concentrated profiles that produce conspicuously large Einstein rings (see Broadhurst & Barkana 08), while observations of weak GL require extended outskirts for affecting numerous background galaxies.

- The weak lensing data are not very constraining yet in view of their considerable uncertainties and possible systematics, but they are progressing by improved control over the redshift distribution of the background galaxies, and over the detailed 3-D structure of the cluster (see Limousin+07; Medezinski+07; Umetsu & Broadhurst 08). Whence we expect progressively sharper evidence for (our) physical profiles.

α-Profiles at Work (II): Galactic Dynamics

- The astrophysical basis of the Sérsic-Einasto model (Work in Progress)

- The empirical Sérsic-Einasto (SE) model

$$\boxed{\rho(r) \propto \hat{r}^{-\tau}\, e^{-\frac{2-\tau}{\eta}\,\hat{r}^{\eta}}}$$

met a considerable success in fitting the profiles of collisionless matter in galaxies: the stellar mass profile in spheroids (see Kormendy+09) and the density profile of galactic DM halos in recent simulations (see Navarro+10).

- On the stellar side, it is well known that deprojecting from the plane of the sky a Sérsic 2-d run $\exp(-s^{1/n})$ with index $n\sim 3$-4 (for normal ellipticals) yields a SE model with $\eta=1/n \sim 0.2$-0.3 and $\tau = 1-1.19/2n+0.22/4n^2 \sim 0.85$ significantly different from 0 and less than 1 (e.g., Prugniel & Simien 97).

α-Profiles at Work (II): Galactic Dynamics

- On the DM side, the density profiles in recent simulations is best described by a SE model with the constraint $\tau<0.9$ and $\eta\sim0.2$-0.3. Still, no agreed understanding is available to explain the value of the SE representations both in the real and virtual world.

- We trace the astrophysical basis of the SE model back to the α-profiles, of which the Sérsic model constitutes a remarkably precise rendition, once its parameters have been fixed to values consistent with the Jeans equation (e.g., the inner slope).

α	1.25	1.27	1.29
Einasto model (Eq. 1 with $\tau = 0$)			
η	0.259	0.226	0.194
SE model (Eq. 1)			
τ	0.630	0.642	0.654
η	0.368	0.326	0.285

OK with stellar obs. and DM sims.

Table from LC10, in prep.

α-Profiles at Work (II): Galactic Dynamics

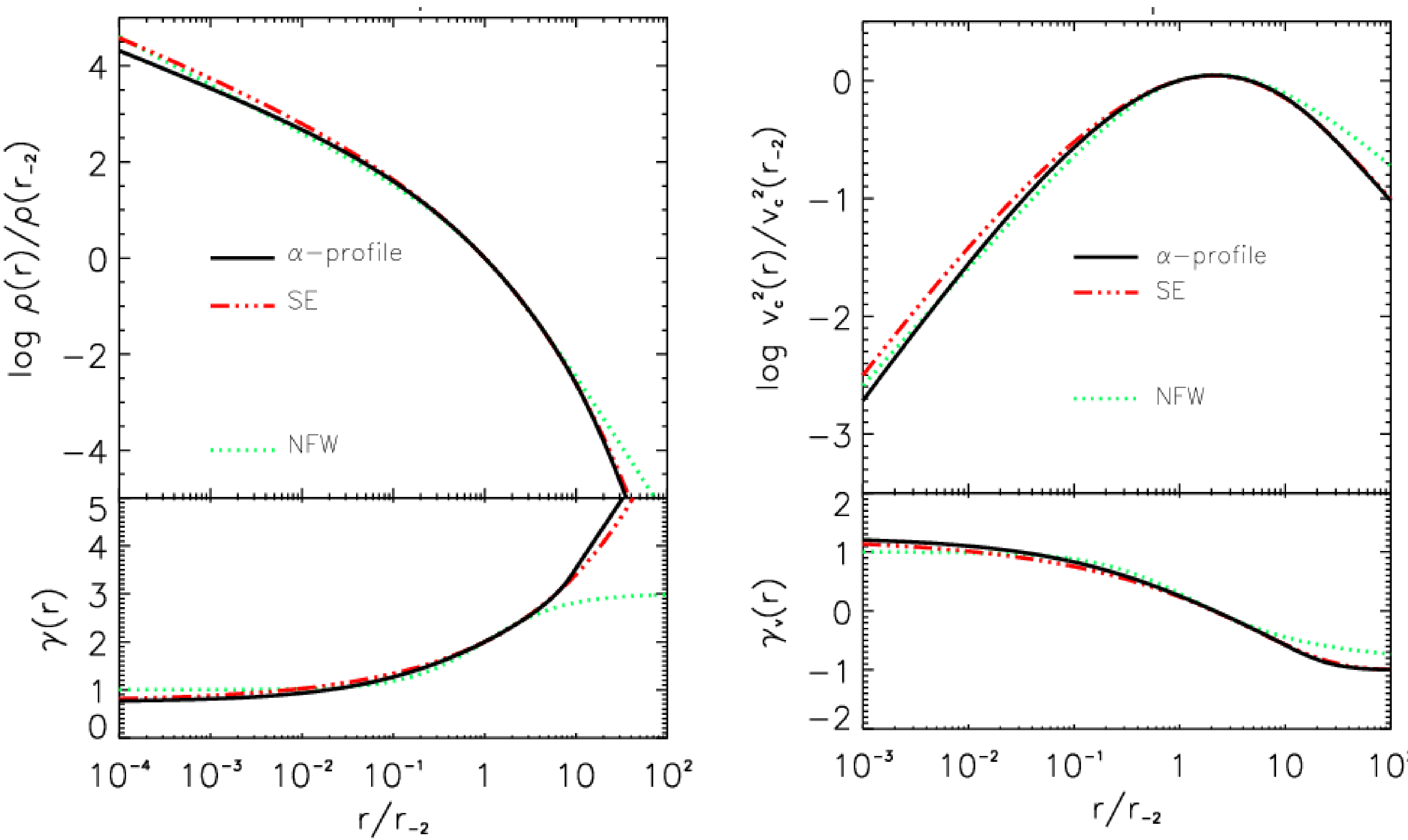

Figure from LC10, in prep.

α-Profiles at Work (III): Astroparticle Physics

Predicting γ-Rays from DM Annihilation at the GC (Lapi+10)

- The γ-ray signal originated via DM annihilations from the Galactic Center depend not only on the microphysics (particle mass/cross section and annihilation channels),

$$\frac{d\Phi_\gamma}{d\Omega} = 3.74\times 10^{-6}\, N_\gamma \left(\frac{\langle \Sigma v\rangle}{10^{-26}\ \mathrm{cm^3\ s^{-1}}}\right) \left(\frac{m_{\rm DM}}{50\,\mathrm{GeV}}\right)^{-2} J(\psi)\quad \mathrm{m^{-2}\ s^{-1}\ sr^{-1}}$$

but also (and even more strongly) on the macroscopic DM distribution via the quantity

$$\boxed{J(\psi) = \int \frac{d\ell}{r_\odot}\, \frac{\rho^2(r)}{\rho^2(r_\odot)}}$$

- We propose the α-profile for the Galaxy halo as a benchmark to gauge in terms of DM annihilations the γ-rays from the GC to be detected with *Fermi*. Such α-profile will be instrumental to derive reliable information about the microscopic nature of DM particle.

α-Profiles at Work (III): Astroparticle Physics

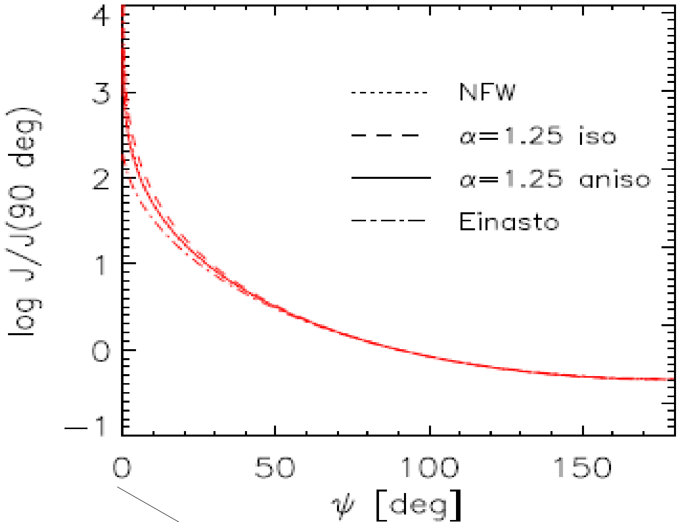

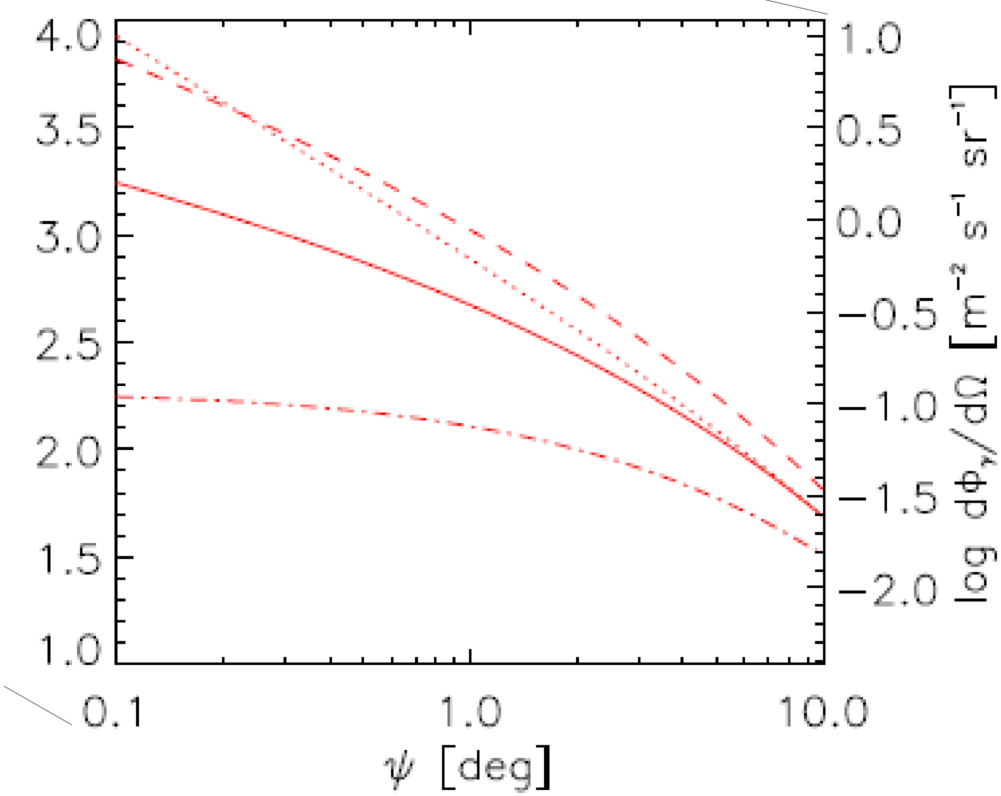

Table 2. Values of the γ-ray flux (in $m^{-2}\ s^{-1}$) for $E_\gamma \geq 200$ MeV.

DM profile	$\Delta\Omega = 10^{-3}$	$\Delta\Omega = 10^{-5}$
NFW	4.7×10^{-4}	4.0×10^{-5}
α iso	5.2×10^{-4}	2.5×10^{-5}
α aniso	2.0×10^{-4}	6.0×10^{-6}
Einasto	4.1×10^{-5}	5.0×10^{-7}

Tables and figures from Lapi+10

α-Profiles at Work (IV): Physics of the ICM

- Basic facts sheet

  - Galaxy Clusters, the largest (R ~ Mpc) and most massive ($M \sim 10^{15}\ M_{sun}$) bound structures in the Universe, are pervaded by huge amounts of hot gas (kT ~ 5 keVs, m ~ M/6) in virial equilibrium within the DM gravitational potential well (see Sarazin88 for a review).

  - This hot gas emits copiuosly in X rays, at luminosities $L_X \sim n^2\, T^{1/2}\, R^3 \sim 10^{44\text{-}46}$ erg s^{-1} mainly via bremms radiation; these correspond to electron densities $n \sim 10^{-3}$ cm^{-3}.

  - Such T and n make the intracluster gas an extremely good plasma, actually the best in the Universe, with ratio of the kinetic to the electrostatic energy being of order

$$10^{12} \sim k_{\rm B}T/e^2 n^{1/3} \equiv G m_p^2/e^2 \times \bar{d}/10\, R \times \mathcal{N}$$

dominated by $N \sim M/m_p \sim 10^{73}$, though $d \sim 10$ cm and $Gm_p^{\,2}/e^2 \sim 10^{-36}$.

α-Profiles at Work (IV): Physics of the ICM

UNIVERSITA' degli STUDI di ROMA TOR VERGATA

- Hydrostatics

  - The equilibrium structure of the ICM within the DM gravitational potential well is regulated by hydrostatic equation (the analogous of the Jeans equation for a collisional gas)

$$\frac{1}{m_p\, n}\,\frac{dp}{dr} = -\frac{G\,M(<r)}{r^2}$$

where the pressure p ~ n $k_B T/\mu$ can be expressed in terms of the ICM entropy (or rather adiabat) $k = k_B T/n^{2/3}$. Remark: the gravitational potential is mainly provided by the DM!

  - The hydrostatic equation can be formally integrated (see Cavaliere+09) to yield

$$\boxed{\bar{T}(\bar{r}) = \bar{k}(\bar{r})\,\bar{n}^{2/3}(\bar{r}) = \bar{k}^{\,3/5}(\bar{r})\left[1 + \frac{2}{5}\,b_R \int_{\bar{r}}^{1} \frac{d\bar{r}'}{\bar{r}'}\,\bar{v}_c^2(\bar{r}')\,\bar{k}^{-3/5}(\bar{r}')\right]}$$

Variables are normalized to their values at r=R, and $b_R \sim \mu m_p v_R^2/k_B T_R$ measures there the ratio of the DM gravitational pull to the ICM random kinetic energy.

α-Profiles at Work (IV): Physics of the ICM

- For handy use in the previous formula, we provide analytic representations of $v_c^2(r)= GM(<r)/r$ in terms of hypergeometric function ${}_2F_1$.

$$\bar{v}_c^{\,2}(\bar{r}) = \bar{r}^{2-s}\,\frac{{}_2F_1[(3-s)/u,\, q,\, 1+(3-s)/u;\, -w\,(c\bar{r})^u]}{{}_2F_1[(3-s)/u,\, q,\, 1+(3-s)/u;\, -w\,c^u]}$$

α	s	u	q
1.25	0.750	0.389	21.465
1.26	0.756	0.399	14.374
1.27	0.762	0.411	10.614
1.28	0.768	0.423	8.316
1.29	0.774	0.436	6.751

- Given that the previous equation has the stand of a theorem in hydrostatics, what actually needs physical modeling is the entropy run k(r), and the boundary condition related to b_R.

More on this, in the next Lecture by Prof. A. Cavaliere...

Summary

- The α-profiles constitute solutions of the Jeans equation with regular boundary conditions and physical features: a finite energy density at the center, monotonically steepening density in the halo body, and a definite mass in the outskirts. If compared with the standard NFW formula, these are flatter at the center and steeper in the outskirts.

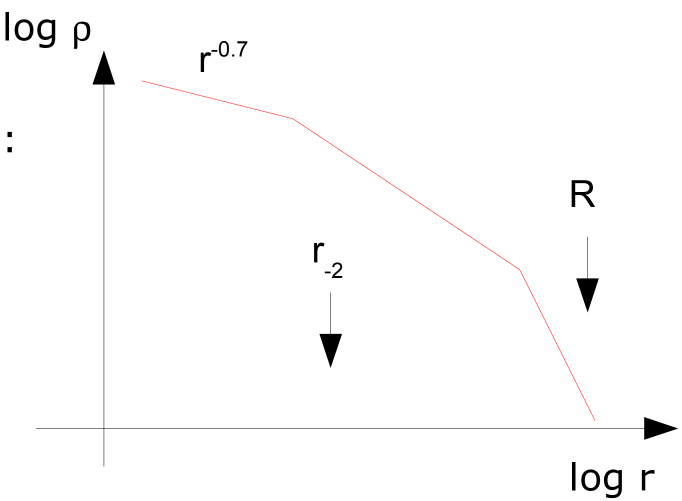

- I have discussed possible applications of the α-profiles to:
  - Gravitational lensing observations
  - Galactic Dynamics
  - Astroparticle physics
  - Physics of the ICM in Galaxy Clusters

- To sum up, I propose the α-profiles to constitute the new benchmarks for the descriptions of the DM equilibria in cosmic structures.

Summary

- <u>My papers related to this subject</u>

  - ***Lapi, A.***, *& Cavaliere, A. 2009, ApJ, 692, 174 [LC09a]*
  - ***Lapi, A.***, *& Cavaliere, A. 2009, ApJL, 695, L125 [LC09b]*
  - ***Lapi, A.,*** *Paggi, A., Cavaliere, A., Lionetto, A., Morselli, A., & Vitale, V. 2010, A&A, 510, 90*
  - ***Lapi, A.***, *& Cavaliere, A. 2010, Adv. In Astron. "Focus Issue on DM", submitted*

DM

  - *Cavaliere, A.,* ***Lapi, A.***, *& Fusco-Femiano, R. 2009, ApJ, 698, 580*
  - *Fusco-Femiano, R., Cavaliere, A., &* ***Lapi, A.*** *2009, ApJ, 705, 1019*
  - ***Lapi, A.***, *Fusco-Femiano, R., & Cavaliere, A. 2010, A&A, in press*

ICM

That's all.
Thank you for the attention!